

Effective macrospin model for $Co_xFe_{3-x}O_4$ nanoparticles: decreasing the anisotropy by Co-doping?

David Serantes,^{1,*} Daniel Faílde,¹ Daniel Baldomir,¹ Beatriz Pelaz,² Pablo del Pino,² and Roy W. Chantrell³

¹*Instituto de Investigaciones Tecnológicas and Applied Physics Department, Universidade de Santiago de Compostela, 15782 Santiago de Compostela, Spain*

²*Centro Singular de Investigación en Química Biolóxica e Materiais Moleculares (CiQUS),*

Departamento de Física de Partículas, Universidade de Santiago de Compostela, 15782 Santiago de Compostela, Spain

³*Department of Physics, University of York, York, YO10 5DD, United Kingdom*

Co-doping of Fe_3O_4 magnetic nanoparticles is an effective way to tailor their magnetic properties. When considering the two extreme cases of the $Co_xFe_{3-x}O_4$ series, i.e. the $x = 0$ and $x = 1$ values, one finds that the system evolves from a negative cubic-anisotropy energy constant, $K_C^- < 0$, to a positive one, $K_C^+ > 0$. Thus, what happens for intermediate x -compositions? In this work we present a very simple phenomenological model for the anisotropy, under the *macrospin* approximation, in which the resultant anisotropy is just directly proportional to the amount of *Co*. First, we perform a detailed analysis on a rather ideal system in which the extreme values have the same magnitude (i.e. $|K_C^-| = |K_C^+|$) and then we focus on the real $Co_xFe_{3-x}O_4$ system, for which $|K_C^+| \sim 18|K_C^-|$. Remarkably, the approach reproduces rather well the experimental values of the heating performance of $Co_xFe_{3-x}O_4$ nanoparticles, suggesting that our simple approach may in fact be a good representation of the real situation. This gives rise to an intriguing related possibility arises: a *Co*-doping composition should exist for which the effective anisotropy tends to zero, estimated here as 0.05.

I. INTRODUCTION

To have particles with similar magnetic moment, shape and size, but different anisotropy, a possible experimental approach is to use Fe_3O_4 magnetite nanoparticles as a base system, and to dope them with e.g. *Mn* or *Co*. In this way, a large variation in the anisotropy constant K is expected while maintaining similar values of the other characteristic parameters. However, from the theoretical point of view, a puzzling question arises regarding the magnetic anisotropy of the system. Consider for example the $Co_xFe_{3-x}O_4$ series as a function of x , which has cubic *negative* anisotropy constant $K_C^- < 0$ on the $x = 0$ extreme of the series (corresponding to Fe_3O_4), but cubic *positive* anisotropy $K_C^+ > 0$ on the other extreme $x = 1$ (i.e. for $CoFe_2O_4$). The question is, what happens for intermediate compositions? What would be the *effective* anisotropy of the Co-doped Fe_3O_4 nanoparticles? The magnetic anisotropy is a key magnetic parameter, particularly for nano-scaled materi-

als at the single-domain range, as it determines the dynamical behaviour[1, 2], efficiency of the magnetic torque [3, 4], or stability of ordered assemblies[5, 6]. Thus, controlling the anisotropy is essential for a broad range of applications as diverse as magnetic recording[7, 8], hyperthermia [9, 10], or magnetic refrigeration[11, 12]. In the following we will develop in this context the *effective* anisotropy from a single-particle (*macrospin* approximation) approach. The article is organized as follows: in Section II we introduce our simple idea to treat this problem; essentially, to approximate the effective anisotropy as dependent on the amount of *Co*-doping (see Figure 1). Then, in Section III we describe the computational model used to study the problem. The results are reported and analysed in Section IV, which contains 2 subsections: firstly, in IV A we analyse the role of the symmetry of the anisotropy, for the ideal case in which $|K_C^-| = |K_C^+|$; then, in IV B the real $Co_xFe_{3-x}O_4$ case is presented. Finally, Section V presents some conclusions and a summary of the work.

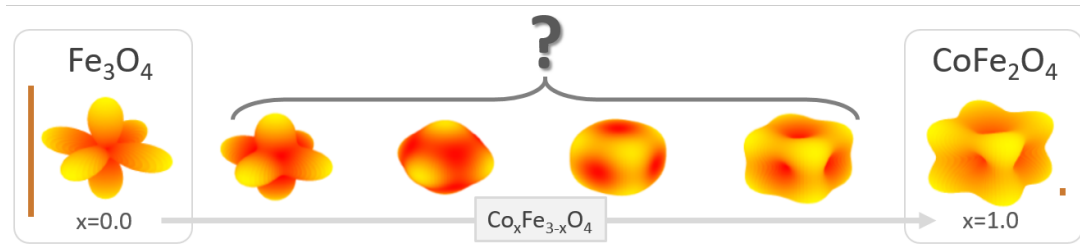


FIG. 1. Schematic illustration of the evolution of the effective anisotropy landscape of $Co_xFe_{3-x}O_4$ nanoparticles as a function of the *Co*-content x . The bars for $x = 0$ and $x = 1$ represent the relative magnitudes of the anisotropy in each case.

II. THE PHENOMENOLOGICAL IDEA

For simplicity, we can envisage a nanoparticle small enough that the magnetic behaviour of the atomic moments is dominated by exchange. In this case, magnetic properties

* E-mail: david.serantes@usc.es

are appropriately described by the *macrospin* approximation -i.e. the particle behaves as a large *supermoment*. For such a nanoparticle, what would be the effect on the net anisotropy of having some *Fe* sites replaced with *Co*? Here we assume firstly that Co^{2+} cations displace octahedral Fe^{2+} sites[13]. Further we assume that, since the anisotropy is a local property, to a first approximation we postulate the coexistence of both types of anisotropies. Then it follows that the net anisotropy is the volume weighted average of the anisotropies of the sites with Fe^{2+} and Co^{2+} cations.

To test this idea we developed a simple theoretical approach in which a positive cubic-anisotropy contribution directly proportional to the *Co*-doping fraction appears onto the cubic-negative anisotropy of the base Fe_3O_4 material. A systematic analysis and characterisation of the resulting magnetic properties of the model is carried out in general terms, and then applied to a particular case: the heating properties of *Co*-doped Fe_3O_4 magnetite nanoparticles as reported experimentally by Fantechi *et al.*[14]. Finally, the intriguing possibility that a small *Co*-doping can lead to a decrease of the particle effective anisotropy is analyzed.

Assuming that the particles are sufficiently small that the inner magnetic moments behave coherently, it seems reasonable to consider that the contribution of every magnetic moment will have a direct influence on the *global* behaviour of the magnetic *supermoment*. Thus, knowing that doping Fe_3O_4 with *Co* adds a positive cubic anisotropy contribution[15], our phenomenological approach gives that the effective particle anisotropy is, in first approximation, proportional to the volume weighted *Co* and *Fe* fractions as

$$K_C = K_C^{Fe_3O_4} \cdot (1-x) + K_C^{CoFe_2O_4} \cdot x, \quad (1)$$

with the nominal bulk anisotropies of Fe_3O_4 and $CoFe_2O_4$ given by $K_C^{Fe_3O_4} = -1.1 \cdot 10^4 J/m^3$ and $K_C^{CoFe_2O_4} = 2.0 \cdot 10^5 J/m^3$, respectively. It is important to emphasize here that while our approach might appear similar to other works tailoring the effective anisotropy by combining soft and hard magnetic materials (e.g. in core/shell geometry, considering the contributions from the different layers to be additive [16, 17]), the essence of the current work is however completely different. What is crucial here is introducing the mixed anisotropies of the *Co* and *Fe* at the atomic level which allows fine-tuning of the anisotropy magnitude and easy-axis orientation, to the best of our knowledge not considered in other approaches. The condition of additivity of the properties arises naturally as a consequence of the uniform magnetisation imposed by the nanoparticle dimensions.

As mentioned in the Introduction section, the simulated particle properties will be based on Fe_3O_4 with progressive *Co* doping. For the sake of simplicity we have assumed that the saturation magnetisation does not vary significantly with *Co* content[18], considering it to have a constant value of $M_S = 480 emu/cm^3$ for all cases. This reasonable assumption allows us to specifically concentrate on the role of the anisotropy. To ensure fully coherent magnetisation reversal we have focused on relatively small spherical nanoparticles of diameter $d = 8.5 nm$; the same values as reported by Fantechi *et al.*[14].

III. COMPUTATIONAL MODEL

Given the small size of the particles, well below the single-domain threshold, we model them as large macrospins with coherent rotation of the inner magnetic moments, as often assumed in theoretical studies of very small magnetic nanoparticles[1, 10, 12]. Thus, the free energy of each particle i is governed by the Zeeman and anisotropy energies as

$$E_i = \vec{\mu}_i \cdot \vec{H} + K_C \left(\alpha^2 \beta^2 + \beta^2 \gamma^2 + \gamma^2 \alpha^2 \right), \quad (2)$$

with $|\vec{\mu}_i| = M_S V_i$, where M_S is the saturation magnetisation and V_i is the particle volume; \vec{H} is the applied magnetic field; K_C is the cubic anisotropy constant and α, β, γ are the cosine directors. The system is considered monodisperse in size, so that the only difference between particles is the orientation of the anisotropy axes and magnetic moment.

The dynamical magnetic response of the particles to the applied magnetic field is described by the Landau-Lifshitz-Gilbert equation using the OOMMF software package[19]. In general the results will consist of simulating $M(H)$ hysteresis loops, both in the quasistatic limit (considering major loops) at zero temperature ($T = 0$); and under rapidly time-varying AC fields (at room temperature) as used in magnetic hyperthermia experiments. The quasistatic simulations were carried out by means of energy minimization; for the dynamical calculations we used the Oxs Extension Module *thetaevolve*[20], to account for thermal effects. It must be noted that to avoid considerations regarding dispersion of particle parameters (size[21], anisotropy[22], etc), we have for the sake of simplicity assumed in all calculations perfectly monodisperse systems. In this regard, given the relatively small particle sizes of the target experiment[14], of about $8.5 nm$ in diameter - thus with a likely significantly bigger heating performance for the larger particles[21, 23], we used the following characteristic size. The simulated size d_{simul} was chosen as the average mean value of each experimental case, $\langle d_{exp} \rangle$, plus 1.5 times the corresponding standard deviation (σ) of each sample, i.e. $d_{simul} = \langle d_{exp} \rangle + 1.5\sigma_{exp}$ to account for the higher weighting of larger particles.

IV. RESULTS AND DISCUSSION

To study the properties of the simple approach described by (1), we shall simulate the magnetic properties of nanoparticles of different $Co_x Fe_{3-x} O_4$ compositions as a function of the x -fraction of *Co* content. However, based on the large difference between the respective anisotropy constants of Fe_3O_4 and $CoFe_2O_4$ (thus with an expected much higher influence of the $K_C > 0$ contribution), for illustrative purposes we will consider at first the ideal case of the anisotropy evolving between K_C^- ($x=0.0$) and K_C^+ ($x=1.0$), with $|K_C^-| = |K_C^+|$. Later, the realistic case of the transition between Fe_3O_4 and $CoFe_2O_4$ alloys will be considered.

Thus, for now we will just consider the effective anisotropy

K_C^{eff} of the ideal situation described by

$$K_C^{eff} = K_C^- \cdot (1-x) + K_C^+ \cdot x, \quad (3)$$

where $K_C^- = -1.1 \cdot 10^4 J/m^3$ and $K_C^+ = 1.1 \cdot 10^4 J/m^3$. By doing so the colors depicted in Figure 1 correspond to the same energy scale, thus making easy to discern the effect of the combined anisotropies. It is important to keep in mind that the different energy geometries are shown for illustrative purposes; otherwise the same geometry with inter-exchanged color scheme would be enough to resemble both positive and

negative anisotropy energies.

A. Ideal case: from K_C^- to K_C^+ , with $|K_C^-| = |K_C^+|$

Firstly, we have simulated the hysteresis loops of the reference cases corresponding to pure $K < 0$ and $K > 0$ (i.e. extreme cases $x = 0$ and $x = 1$). Typical hysteresis loops for various angles of field direction are shown in Figure 2, for two different rotation cross-sections: parallel to the XZ plane ($\varphi = 0^\circ$), and rotated ($\varphi = 15^\circ$) around the Z direction.

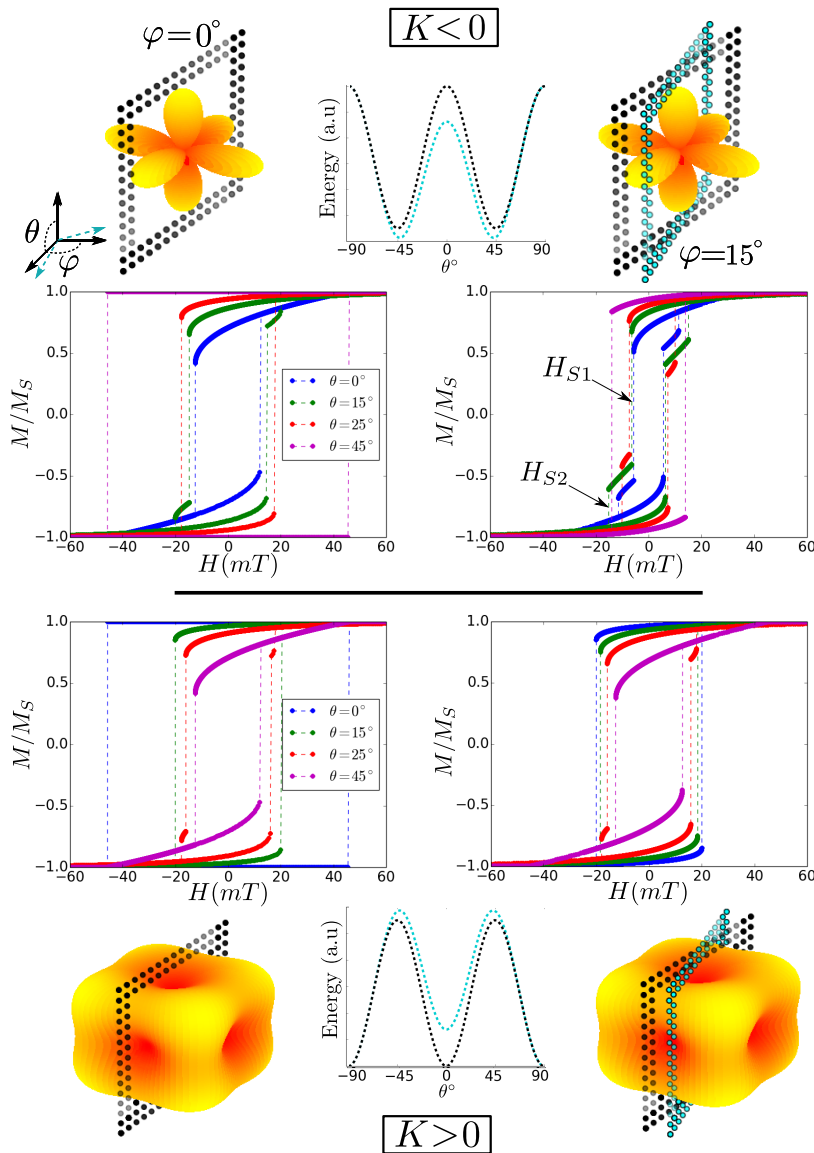


FIG. 2. Hysteresis loops corresponding to the extreme cases $x = 0$ ($K_C < 0$, top panel) and $x = 1$ ($K_C > 0$, bottom panel), for the ideal case $|K_C^-| = |K_C^+|$ (as described by equation (3)). For each case the loops correspond to rotation within the XZ plane ($\varphi = 0^\circ$; left panel) or at $\varphi = 15^\circ$ around the Z direction (right panel), to show the different symmetries throughout the loop. The magnetisation switching can be a one- or a two-step process (switching fields H_{S1} , H_{S2}).

The results displayed in Figure 2 are similar -but of opposite trends- for both signs of anisotropy. Depending on the orientation between field and anisotropy easy axes, the magnetisation

will undergo one or two switching events, and also exhibit different area and coercivity. For example, hysteresis loops for field variation along $\theta = 0^\circ$ have a strong dependence on the

sign of the anisotropy. For $K > 0$ the magnetisation starts in an easy direction giving a square loop and large coercivity, whereas for $K < 0$ the magnetisation starts in a hard direction resulting in a rounded loop with reduced area and coercivity.

Having shown and analyzed the known extreme cases of $x = 0$ and $x = 1$, we now proceed in a similar way (simulation

of angular-dependent hysteresis loops) for mixed-anisotropy compositions as described by equation (3). To compare the different cases we have focused on the angular-dependence of the switching fields (H_S), for the same illustrative cases of $\varphi = 0^\circ$ and $\varphi = 15^\circ$ of Figure 2. The results are summarized in Figure 3.

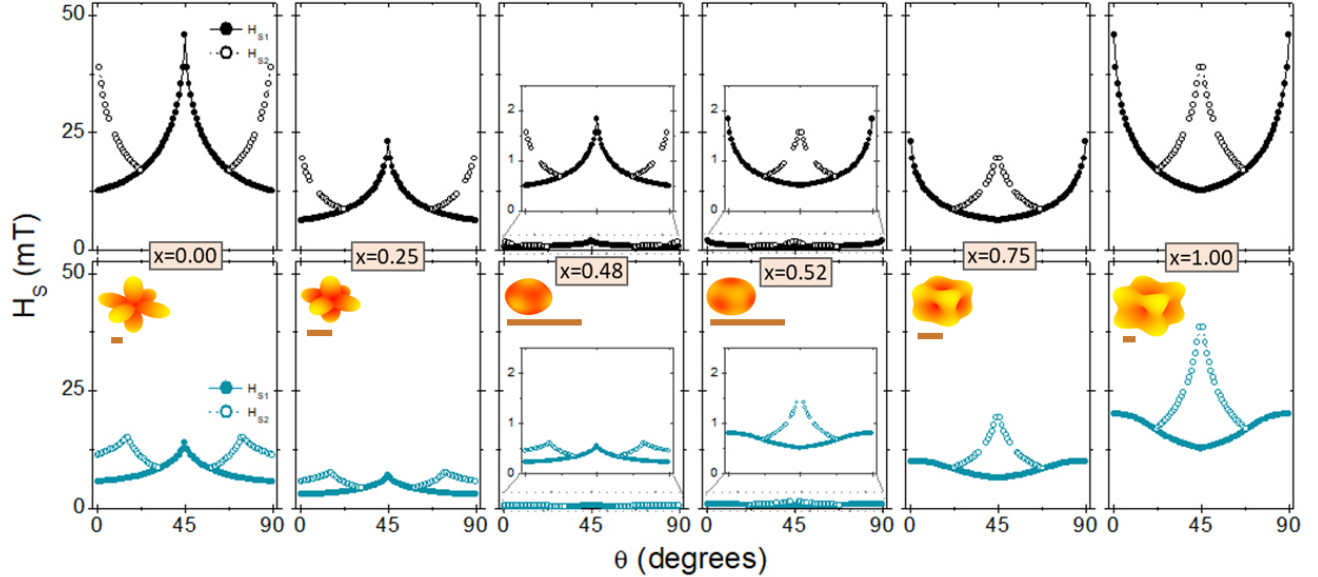


FIG. 3. Angular dependence of the switching fields (as described in Figure 2, for different fractions of positive and negative anisotropy constants). Top and bottom panels for each doping case correspond, respectively, to the $\varphi = 0^\circ$ and $\varphi = 15^\circ$ cases described in Figure 2. The yellow-orange drawings stand for the corresponding energy landscape of each x fraction, with the close small bar illustrating the different energy scales.

The first main feature observed in Figure 3 is that while the overall shape of the H_S vs. θ is quite similar for all x cases, the absolute values rapidly decrease and tend to zero close to the 50% composition (note that the choice of $x = 0.48$ and $x = 0.52$ was made specifically to illustrate this observation). The second main relevant aspect observed in Figure 3 is that the apparent symmetry in the magnetic properties around the $x = 0.50$ value observed for the case $\varphi = 0^\circ$ does not hold for the case of $\varphi = 15^\circ$. This is due to the different symmetry of the energy landscapes of the $K_C < 0$ and $K_C > 0$ cases (with 6 or 8 easy directions, respectively), which results in energy barriers of $K_C V/12$ or $K_C V/4$, respectively[24]. In order to weight the relative importance of such differences and considering the likely random orientation of a real sample in space, we have simulated the average properties of a system with randomly distributed easy axis directions for this ideal situation described by Eq. (3). The results are displayed in Figure 4.

The main panel within Figure 4 shows various hysteresis loops, including the theoretically well known extreme cases of pure $K_C < 0$ ($x = 0$) and $K_C > 0$ ($x = 1$). A detailed analysis of those indicates that the theoretical values of coercive field (H_c) and remanence (M_r) are well reproduced: for $K_C < 0$ we obtain $H_c = 0.20H_K$, where $H_K = 2K/M_S$, and $M_r = 0.87M_S$;

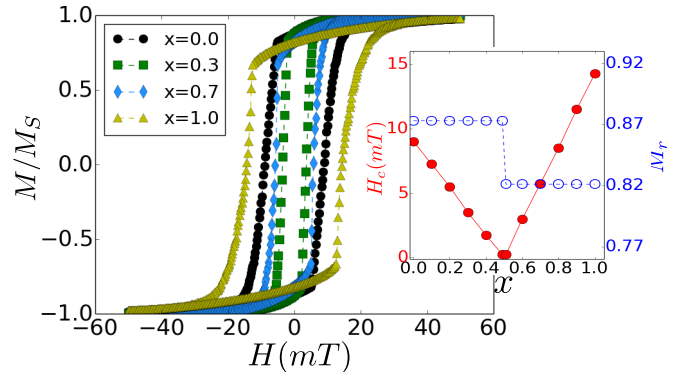


FIG. 4. Main panel: $M(H)$ hysteresis loops (corresponding to a randomly dispersed system), for various illustrative $\text{Co}_x\text{Fe}_{3-x}\text{O}_4$ compositions; inset: detailed evolution of the coercive field, H_c , and remanence, M_r , as a function of x .

and $K_0 > 0$ we find $H_c = 0.32H_K$ and $M_r = 0.82M_S$, as theoretically described by Usov *et al.*[25]. Such good agreement adds further support to our numerical results.

Regarding the combination of anisotropies, two main characteristics are observed: on the one hand, H_c shows a markedly linear initial decrease until reaching zero at about

$x = 0.5$, followed by a subsequent increase (also essentially linear, but of different slope); the extreme values in both cases correspond to the theoretical ones reported by Usov *et al.*[25] described earlier on. Since the coercive field is directly proportional to the anisotropy (no shape or interparticle interactions are present) this means that the approach predicts that *the combination of opposite-symmetry anisotropies may lead to the cancellation of the effective total anisotropy*. We shall come back to this aspect later on. On the other hand and regarding the remanence, we also observed a two-regime behaviour but in this case of completely different features: M_R is a bi-valued constant with the threshold at $x = 0.5$, reaching the corresponding extreme cases for smaller and larger values as reported previously.

B. The real $Co_xFe_{3-x}O_4$ case: from $K_C^- = -1.1 \cdot 10^4 J/m^3$ to $K_C^+ = 2.0 \cdot 10^5 J/m^3$

Now that we have already analyzed the general properties demonstrated by the simple approach summarized by Eq. (3), we investigate the behavior of the real $Co_xFe_{3-x}O_4$ system as described by Eq. (1). As mentioned in the Introduction, our goal is to study the hyperthermia performance of the $Co_xFe_{3-x}O_4$ particles reported by Fantechi *et al.*[14]. Thus, we simulated dynamic hysteresis loops for the experimental particle properties under the same field conditions, assigning to the effective anisotropy the value obtained from Eq. (1). Some representative dynamical curves are shown in Figure 5, where also the quasistatic curves of the $x = 0.0$ and $x = 1.0$ limit cases are displayed for illustrative purposes.

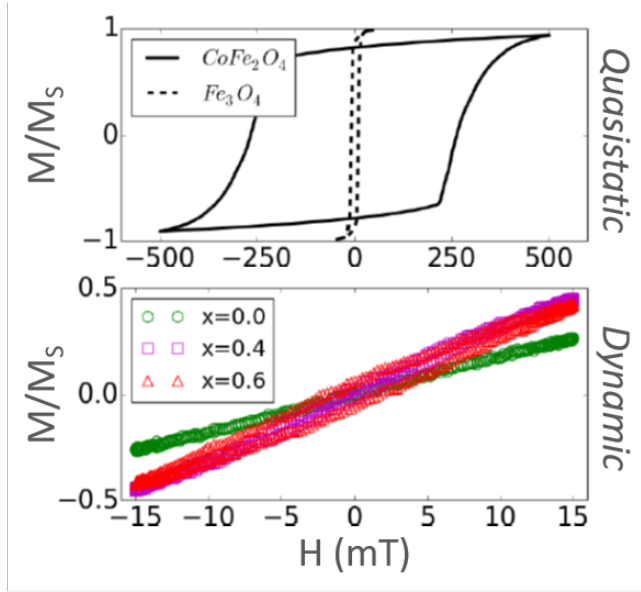


FIG. 5. Top panel: quasistatic $M(H)$ curves of the extreme cases of the series. Bottom panel: several dynamic $M(H)$ loops corresponding to the experimental conditions reported in Ref. [14] (frequency 183 kHz; field amplitude 12 kA/m; temperature 300 K).

The results displayed in Figure 5 show that while a large

difference depending on the composition is observed in the quasistatic curves (top panel), for the dynamical conditions (bottom panel) the curves become apparently very similar. However, the numerical evaluation of the hysteresis loop area of the dynamical loops indicate that there are in fact substantial differences. The loop area is used to estimate the *Specific Absorption Rate* (SAR), i.e. the heating capability of the particles, usually defined as $SAR = area \times frequency$. The corresponding SAR values are summarized in Figure 6, showing good agreement between experiments and simulations. Such good agreement undoubtedly provides strong support to the simple effective anisotropy macrospin approach proposed here.

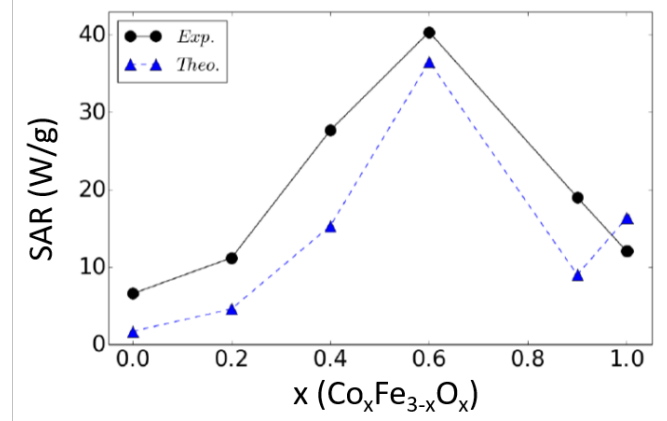


FIG. 6. Comparison between the experimentally measured SAR values reported in Ref. [14] (black dots), and the ones obtained from the simulations (blue triangles).

Having said that, the question posed in view of Figure 4 still holds: would it be possible to lower the (already quite small) anisotropy of Fe_3O_4 nanoparticles by doping with Co? This intriguing question is answered in Figure 7, which suggests that a small *Co*-doping (of about 5%) would lead to a suppression of the effective anisotropy.

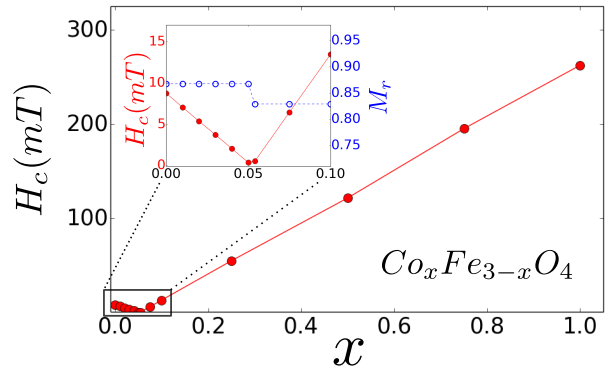


FIG. 7. Predicted *Co*-doping dependence of the coercive field for $Co_xFe_{3-x}O_4$ nanoparticles according to Eq. (1).

V. CONCLUSIONS

We have considered theoretically, under the *macrospin* approximation, the evolution of the effective magnetic anisotropy of the $Co_xFe_{3-x}O_4$ series as a function of x , from the extreme cases of negative cubic-anisotropy of Fe_3O_4 , to the positive cubic-anisotropy of $CoFe_2O_4$. Our phenomenological model assumes the Co -doping to result in an increasing $K_C > 0$ contribution onto the $K_C < 0$ Fe_3O_4 parent phase, which changes continuously both the magnitude and the symmetry of the net anisotropy. On this basis we have developed a simple model for the effective anisotropy of the macrospin in which $K_C < 0$ and $K_C > 0$ coexist in combination, directly proportional to the fraction of Co present in the Fe_3O_4 phase. Applying this model to an experimental study on hyperthermia performance of $Co_xFe_{3-x}O_4$ nanoparticles [14] we obtain a remarkably good agreement, which suggests that our simple assumptions may be reasonable. Interestingly, a side conclusion of our approach is that it predicts that a small Co -doping would lead to a decrease, and even the disappearance of the effective anisotropy, a quite unexpected result. It is the

subject of future work to investigate such an intriguing possibility. However, we note that this may be complicated to demonstrate experimentally due to the required conditions, in particular it would be necessary to achieve highly spherical samples to remove shape-anisotropy effects, which for such small anisotropy could be very relevant and even dominate over the magnetocrystalline contribution[26]).

VI. ACKNOWLEDGEMENTS

We acknowledge the Centro de Supercomputacion de Galicia (CESGA) for the computational resources. This research was partially supported by the Consellería de Educación Program for Development of a Strategic Grouping in Materials (AeMAT) at the Universidade de Santiago de Compostela (ED431E2018/08, Xunta de Galicia). D.S. also acknowledges Xunta de Galicia for financial support under the I2C Plan. Financial support of an International Exchanges grant (IE160535) of the Royal Society is gratefully acknowledged.

-
- [1] K. L. Livesey, N. R. Ruta, S. Anderson, D. Baldomir, R. W. Chantrell, and D. Serantes, *Sci. Rep.* **8** (2018).
- [2] D. Serantes, D. Baldomir, M. Pereiro, C. E. Hoppe, F. Rivadulla, and J. Rivas, *Phys. Rev. B* **82**, 134433 (2010).
- [3] R. Chantrell, B. Tanner, and S. Hoon, *Journal of Magnetism and Magnetic Materials* **38**, 83 (1983).
- [4] D. Serantes, R. Chantrell, H. Gavián, M. P. Morales, O. Chubykalo-Fesenko, D. Baldomir, and A. Satoh, *Phys. Chem. Chem. Phys.* **20**, 30445 (2018).
- [5] D. Serantes, D. Baldomir, M. Pereiro, B. Hernando, V. M. Prida, J. L. S. Llamazares, A. Zhukov, M. Ilyn, and J. González, *Journal of Physics D: Applied Physics* **42**, 215003 (2009).
- [6] A. Arora, L. C. Phillips, P. Nukala, M. Ben Hassine, A. A. Ünal, B. Dkhil, L. Balcells, O. Iglesias, A. Barthélémy, F. Kronast, M. Bibes, and S. Valencia, *Phys. Rev. Materials* **3**, 024403 (2019).
- [7] H. J. Richter, A. Lyberatos, U. Nowak, R. F. L. Evans, and R. W. Chantrell, *Journal of Applied Physics* **111**, 033909 (2012).
- [8] C. J. Aas, P. J. Hasnip, R. Cuadrado, E. M. Plotnikova, L. Szunyogh, L. Udvardi, and R. W. Chantrell, *Phys. Rev. B* **88**, 174409 (2013).
- [9] I. Conde-Leboran, D. Baldomir, C. Martínez-Boubeta, O. Chubykalo-Fesenko, M. del Puerto Morales, G. Salas, D. Cabrera, J. Camarero, F. J. Teran, and D. Serantes, *The Journal of Physical Chemistry C* **119**, 15698 (2015).
- [10] S. Ruta, R. Chantrell, and O. Hovorka, *Sci. Rep.* **5** (2015).
- [11] P. J. von Ranke, N. A. de Oliveira, E. J. R. Plaza, V. S. R. de Sousa, B. P. Alho, A. M. G. Carvalho, S. Gama, and M. S. Reis, *Journal of Applied Physics* **104**, 093906 (2008).
- [12] D. Serantes, V. Vega, W. O. Rosa, V. M. Prida, B. Hernando, M. Pereiro, and D. Baldomir, *Phys. Rev. B* **86**, 104431 (2012).
- [13] J. C. Slonczewski, *Phys. Rev.* **110**, 1341 (1958).
- [14] E. Fantechi, C. Innocenti, M. Albino, E. Lottini, and C. Sangregorio, *Journal of Magnetism and Magnetic Materials* **380**, 365 (2015).
- [15] L. Marcano, D. Munoz, R. Martin-Rodriguez, I. Orue, J. Alonso, A. Garcia-Prieto, A. Serrano, S. Valencia, R. Abrudan, L. Fernandez-Barquin, A. Garcia-Arribas, A. Muela, and M. L. Fdez-Gubieda, *The Journal of Physical Chemistry C* **122**, 7541 (2018).
- [16] Q. Zhang, I. Castellanos-Rubio, R. Munshi, I. Orue, B. Pelaz, K. I. Gries, W. J. Parak, P. del Pino, and A. Pralle, *Chemistry of Materials* **27**, 7380 (2015).
- [17] M. S. Carrião and A. F. Bakuzis, *Nanoscale* **8**, 8363 (2016).
- [18] J. M. Byrne, V. S. Coker, S. Moise, P. L. Wincott, D. J. Vaughan, F. Tuna, E. Arenholz, G. van der Laan, R. A. D. Patrick, J. R. Lloyd, and N. D. Telling, *Journal of The Royal Society Interface* **10** (2013).
- [19] M. Donahue and D. Porter, "Oommf user's guide, version 1.0, interagency report nistir 6376, national institute of standards and technology, gaithersburg, md (sept 1999)," <http://math.nist.gov/oommf> (2018).
- [20] O. Lemcke, "Models finite temperature via a differential equation of the langevin type," http://www.nanoscience.de/group_r/stm-spstm/projects/temperature/download.shtml (2018).
- [21] C. Munoz-Menendez, I. Conde-Leboran, D. Baldomir, O. Chubykalo-Fesenko, and D. Serantes, *Phys. Chem. Chem. Phys.* **17**, 27812 (2015).
- [22] C. Munoz-Menendez, D. Serantes, J. M. Ruso, and D. Baldomir, *Phys. Chem. Chem. Phys.* **19**, 14527 (2017).
- [23] C. Munoz-Menendez, I. Conde-Leboran, D. Serantes, R. Chantrell, O. Chubykalo-Fesenko, and D. Baldomir, *Soft Matter* **12**, 8815 (2016).
- [24] R. Yanes, O. Chubykalo-Fesenko, H. Kachkachi, D. A. Garanin, R. Evans, and R. W. Chantrell, *Phys. Rev. B* **76**, 064416 (2007).
- [25] N. Usov and S. Peschany, *Journal of Magnetism and Magnetic Materials* **174**, 247 (1997).
- [26] N. A. Usov, *Journal of Applied Physics* **107**, 123909 (2010).